

Soft Matter

Accepted Manuscript



This is an *Accepted Manuscript*, which has been through the Royal Society of Chemistry peer review process and has been accepted for publication.

Accepted Manuscripts are published online shortly after acceptance, before technical editing, formatting and proof reading. Using this free service, authors can make their results available to the community, in citable form, before we publish the edited article. We will replace this *Accepted Manuscript* with the edited and formatted *Advance Article* as soon as it is available.

You can find more information about *Accepted Manuscripts* in the [Information for Authors](#).

Please note that technical editing may introduce minor changes to the text and/or graphics, which may alter content. The journal's standard [Terms & Conditions](#) and the [Ethical guidelines](#) still apply. In no event shall the Royal Society of Chemistry be held responsible for any errors or omissions in this *Accepted Manuscript* or any consequences arising from the use of any information it contains.

Directed Peptide Amphiphile Assembly Using Aqueous Liquid Crystal Templates in Magnetic Fields

Pim van der Asdonk^{a,c,‡}, Masoumeh Keshavarz^{a,b,c,‡}, Peter C.M. Christianen^{b,c}, Paul H.J. Kouwer^{*a,c}

^a Department of Molecular Materials, Radboud University, Heyendaalseweg 135, 6525 AJ Nijmegen, The Netherlands

* E-mail: p.kouwer@science.ru.nl

^b High Field Magnet Laboratory (HFML - EMFL), Radboud University, Toernooiveld 7, 6525 ED Nijmegen, The Netherlands

^c Institute for Molecules and Materials, Radboud University, Heyendaalseweg 135, 6525 AJ Nijmegen, The Netherlands

[‡] These authors contributed equally.

Abstract

An alignment technique based on the combination of magnetic fields and a liquid crystal (LC) template uses the advantages of both approaches: the magnetic fields offer non-contact methods that apply to all sample sizes and shapes, whilst the LC templates offer high susceptibilities. The combination introduces a route to control the spatial organization of materials with low intrinsic susceptibilities. We demonstrate that we can unidirectionally align one such material, peptide amphiphiles in water, on a centimeter scale at a tenfold lower magnetic field by using a lyotropic chromonic liquid crystal as a template. We can transform the aligned supramolecular assemblies into optically active π -conjugated polymers after photopolymerization. Lastly, by reducing the magnetic field strength needed for addressing these assemblies, we are able to create more complex structures by initiating self-assembly of our supramolecular materials under competing alignment forces between the magnetically induced alignment of the assemblies (with a positive diamagnetic anisotropy) and the elastic force dominated alignment of the template (with a negative diamagnetic anisotropy), which is directed orthogonally. Although the approach is still in its infancy and many critical parameters need optimization, we believe that it is a very promising technique to create tailor-made complex structures of (aqueous) functional soft matter.

Introduction

Self-assembly in aqueous solutions is an excellent approach to fabricate functional materials that can interface with biological and biochemical processes, for instance within sensing devices.¹⁻³ Controlling the macroscopic organization (such as micropatterns and alignment) of such aqueous supramolecular materials across multiple length scales is essential for device performance⁴⁻⁷, but remains a major challenge to date. Over the years, many techniques have been developed to control the spatial organization of aqueous self-assembling materials, including photolithography^{8,9}, soft lithography^{9,10}, electrospinning¹¹⁻¹³, electric fields¹⁴⁻¹⁷ and magnetic fields¹⁸⁻²⁰. All these techniques have demonstrated their use in specific situations, but they also suffer from limitations that are often directly associated to the organization of aqueous soft materials. For instance, such materials frequently display a low susceptibility and incompatibility to strong electric fields. Also complex pattern formation of these structures over multiple length scales on a wide range of surfaces is very challenging.

We recently explored liquid crystal templating as a tool to direct the spatial organization of supramolecular materials in water.²¹ This approach offers a number of unique advantages: *(i)* LC templating does not depend on delicate molecular interactions and is therefore suitable to organize a wide range of soft materials; *(ii)* the liquid crystal (LC) template itself is highly susceptible to external stimuli and is readily manipulated to generate complex patterns; *(iii)* after alignment, organization and optional post-modification, the LC template can be removed, leaving only the aligned functional material on the substrate. LC templating has been applied successfully to align organic²²⁻³¹ and, to a lesser extent, aqueous functional materials³²⁻³⁷. Mostly, surface interactions were used to control the alignment of aqueous soft matter, although one example of carbon nanotube alignment in a magnetic field aligned lyotropic liquid crystal was published³².

Here, we use the advantages of LC templating and combine them with the unique features of magnetic field alignment, which is an intrinsic contact-free alignment technique (no specific directing surfaces needed). We demonstrate that this approach allows for the formation of complex patterns by cleverly exploiting the differences in sign and strength of the diamagnetic anisotropies of the LC template and the dispersed soft material.

To demonstrate this concept, we aligned and patterned peptide amphiphiles (**PA**) in a lyotropic chromonic liquid crystal (LCLC) template in a magnetic field. In an aqueous LCLC template solution, **PA** self-assembles into nanometer-wide fibers and progressively bundles into hierarchical micron to millimeter-sized structures. We show that we need a tenfold lower magnetic field to align these amphiphilic bundles over a centimeter range in the presence of the magnetically responsive LCLC template. Post-modification provides an easy method to introduce functionality and dimensional stability to the structures; the latter allows for removal of the template by washing. The reduction of the magnetic field alignment threshold opens up a window for the creation of more complex

structures at high magnetic fields. Here, we anticipate a competition between the magnetically induced alignment of the **PA** assemblies (with a positive diamagnetic anisotropy) and the elastic force dominated alignment of the template (with a negative diamagnetic anisotropy), which is directed orthogonally.

Materials and methods

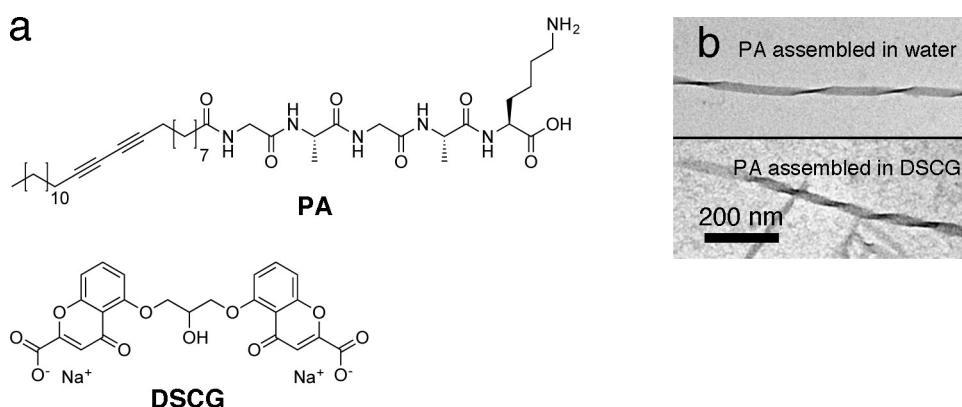


Figure 1. Molecular structures (a) of **PA** and DSCG. Transmission electron microscopy (b) images of **PA** assembled in water (top) and in nematic DSCG in water (bottom), showing in both cases a fibrous twisted beta-sheet structure.

The peptide amphiphile that we use are self-assembling supramolecular materials which have shown a lot of promise in both biomedical engineering and sensing applications.³⁸⁻⁴⁵ Its synthesis and characterization has been reported before.^{21,45} The amphiphile consists of a 25 carbon hydrophobic tail and a GAGAK hydrophilic head section (**Figure 1a**). In both water and in nematic DSCG at room temperature, **PA** self-assembles due to hydrophobic-hydrophilic interactions, forming long 1D beta-sheet fibers (Figure 1b). In water, these beta-sheets form isotropic assemblies at larger length scales.²¹ Furthermore, **PA** was functionalized with a diacetylene-moieity, which allows us to crosslink these materials by a topological photopolymerization step, resulting in a greatly improved mechanical stability and a strong chromatic response due to the π -conjugated backbones. For device applications, such as in tissue engineering^{38,39,41,42} and molecular electro-optics⁴⁰ controlled long range ordering of these materials is essential. Macroscopic alignment was realized with shear flow^{38,40,46}, electrospinning¹³ and a high magnetic field approach^{18,19}, whereas multi-length scale control was accomplished using soft lithography⁴⁷ and recently with an LCLC template on photopatterned substrates²¹. The high magnetic field experiments showed that, at sufficient field strengths, **PA** assemblies align with their long axis parallel to the magnetic fields (with the hydrogen bonds parallel and the alkyl chains perpendicular to the field)^{18,48}. The magnetic alignment of such materials depends on the anisotropy of the diamagnetic susceptibility and the strength of the applied field. We calculated a value of $\Delta\chi = \Delta\chi_{\parallel} - \Delta\chi_{\perp} \approx -611 \cdot 10^{-12} \text{ m}^3 \text{ mol}^{-1}$ for the molar diamagnetic susceptibility for **PA** (see Supporting Information). The number is negative (i.e. **PA** will align with the molecular axis

perpendicular to the field, but 1D assemblies will align parallel to the field) and small, which confirms that even for large assemblies high magnetic fields are necessary to obtain alignment.

We chose disodium cromoglycate (DSCG) as a lyotropic chromonic liquid crystal (LCLC) template to direct the organization of **PA** in magnetic fields. DSCG is a rigid plank-like molecule that consists of an aromatic core with water-solubilizing groups on the periphery (Figure 1a). In water, the molecules stack face-to-face in columnar aggregates due to π - π stacking and hydrophobic interactions, and at certain concentrations and temperatures, these aggregates form nematic and smectic phases.⁴⁹ Recently, nematic DSCG solutions have been used to template the organization of motile bacteria³⁵⁻³⁷ and the alignment of carbon nanotubes³⁴ and peptide amphiphiles²¹.

The molar diamagnetic susceptibility of DSCG is positive and much larger. We calculated a value of $\Delta\chi = \chi_{\parallel} - \chi_{\perp} \approx 1226 \cdot 10^{-12} \text{ m}^3 \text{ mol}^{-1}$. Now the molecules will order with their long axis parallel to the field and the 1D assemblies will order in a plane perpendicular to it. As the concentration DSCG is much higher than the concentration PA, one expects that DSCG can be aligned at much lower field strengths. Indeed, experimentally was found that magnetic fields as low as 0.7 T^{50,51} are sufficient to align a nematic solution of DSCG. By placing DSCG solutions in a confined space (such as in a glass cell of a several microns spacing), the stacks are forced to align in-plane and perpendicular to the magnetic field vector. The ability of DSCG to act as an aqueous anisotropic solvent which can direct other dispersed materials, while also having relatively high magnetic susceptibilities, makes this particular template an excellent material to control the structural organization of **PA**s, but potentially a much wider range of aqueous functional soft materials using magnetic fields.

Results and discussion

Unidirectional aligned arrays of π -conjugated peptide amphiphiles

To create unidirectionally aligned arrays of dichromic **PA**s, we filled glass cells (23 micron spacing) with a mixture of **PA** (0.026 wt%) and DSCG (13.7 wt%) in milli-Q. The glass cells were sealed with epoxy glue to prevent water evaporation and after 1 hour of drying, the cells were loaded in the magnetic field setup. The temperature was increased to 80 °C after which a magnetic field ($\mathbf{B} = 2$ T) was turned on. With the magnetic field on, the sample was cooled to room temperature over a period of 40–60 minutes. Subsequently, the magnet field was switched off and the sample was removed. Polarized optical microscopy (POM) was used to investigate the assembly and alignment of **PA** and DSCG.

Figure 2 shows microscopy images of **PA** and DSCG after cooling to room temperature in the presence of a 2 T magnetic field. DSCG forms a unidirectionally aligned monodomain over centimeter dimensions (Figure 2a). The DSCG stacks are aligned in-plane and perpendicular to the direction of the magnetic field, as confirmed by analyzing the optical appearance after inserting a

quarter wave plate between analyzer and sample in the POM stage (Figure S1). Over the same centimeter length scales, OM reveals extended fibrous bundles aligned (Figure 2b), which are macroscopically aligned self-assembled **PA** fibers, oriented parallel to the DSCG template and thus perpendicular to the magnetic field direction. Furthermore, in many locations, spindle-like structures are observed (Figure 2c) from which aligned fibrous bundles emerge. We believe that these spindles are nucleation sites of the initial **PA** fibers formation from which (aligned) fiber growth was initiated later in the cooling process.

After assembly in the magnetic field, a photopolymerization step (initiated by leaving the glass cells uncovered on a lab table for several hours or by a 10 minute illumination with a conventional UV-lamp) crosslinked the aligned **PA** bundles, which consequently became bright blue in color due to the π -conjugated backbone structure (Figure 2b,c). At this stage, the cells were opened and DSCG was washed away, leaving mechanically stable **PA** bundles (as a result of the photopolymerization process) organized unidirectionally on the substrate. Scanning electron microscopy (SEM, Figure 2d) shows massive arrays of fibrous **PA** bundles unidirectionally aligned perpendicular to the magnetic field. Control experiments demonstrated the role of the liquid crystalline template. Without DSCG present, we found no macroscopic fibre alignment for either the samples grown in the absence (Figure S2) or in the presence (Figure S3) of the magnetic field. Mixtures of **PA** in DSCG in the absence of a magnetic field showed random in-plane LCLC alignment, resulting the formation of disordered fibres (Figure S4). We found that the applied magnetic field has no observable influence on the observed **PA** bundle morphology; the microscopy images of mixtures of **PA** and DSCG assembled in the absence of a magnetic field (Figure S5) show similar **PA** assembly morphologies, compared to when **PA** is assembled in a DSCG template with a magnetic field applied (Figure 2).

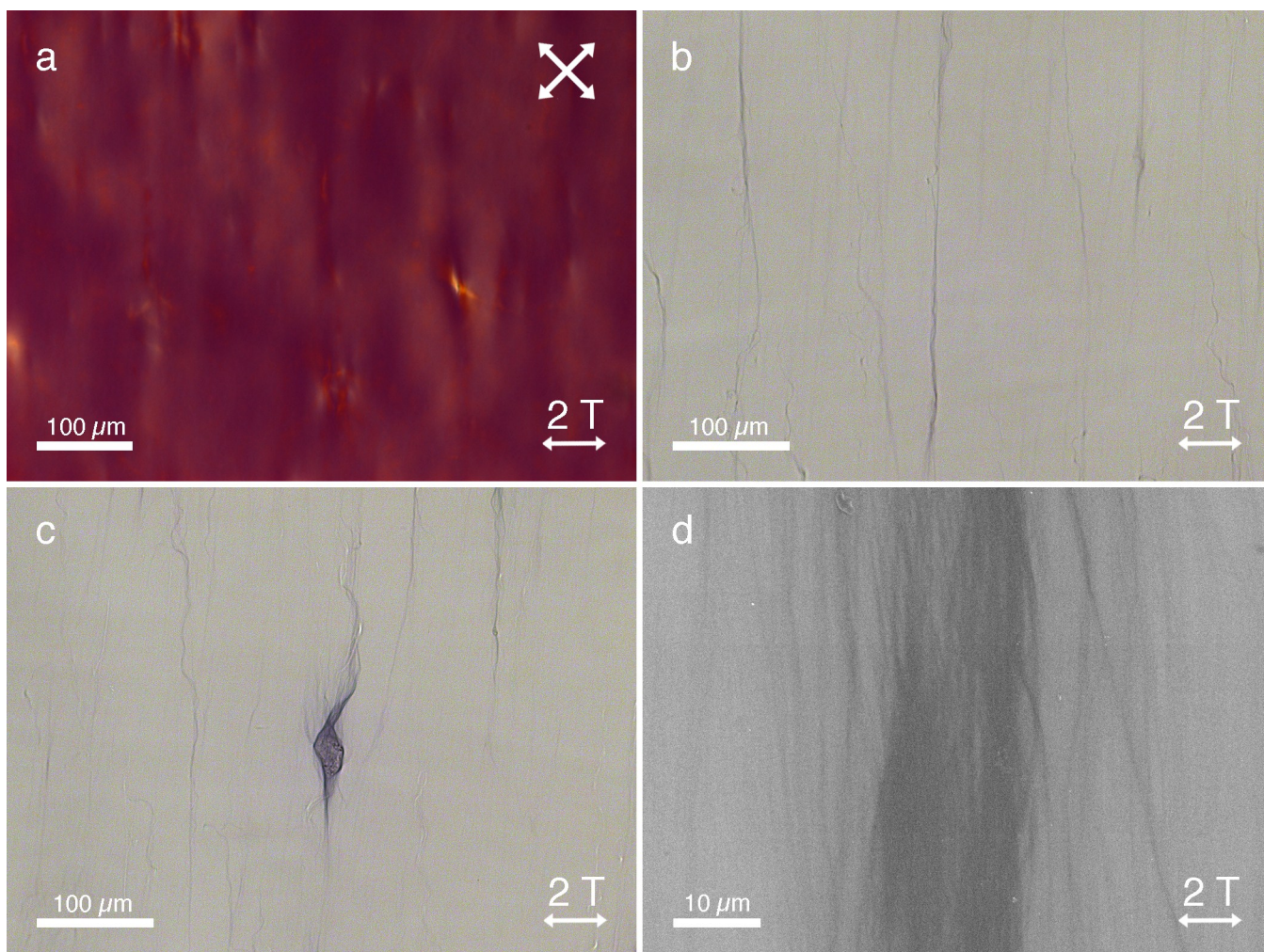


Figure 2. Microscopy images of **PA** (0.026 wt%) in a nematic DSCG template (13.7 wt% in milli-Q) after alignment in a 2 T magnetic field. POM image (a) shows a unidirectionally aligned monodomain of DSCG. OM image (b) shows photopolymerized **PA** bundles aligned along the direction of DSCG template. Image (c) shows an example of the spindle-like structures also present in the DSCG template. After opening the cell and washing away DSCG, scanning electron microscopy (SEM) image (d) shows an aligned photopolymerized **PA** bundle in greater detail. White double-sided arrows indicate the direction of the applied magnet field.

Due to the macroscopic unidirectional alignment of the π -conjugated backbones of these amphiphilic polydiacetylenes, strong linear dichroism is induced (**Figure 3**). Linearly polarized light parallel to the backbone of the **PA** assemblies is strongly absorbed (Figure 3a), whereas the absorption of linearly polarized light oriented perpendicular to the assemblies is drastically reduced (Figure 3b). Additionally, the polymerized assemblies are very stable in demanding conditions (Figure S6), even at temperatures as high as 90 °C.²¹

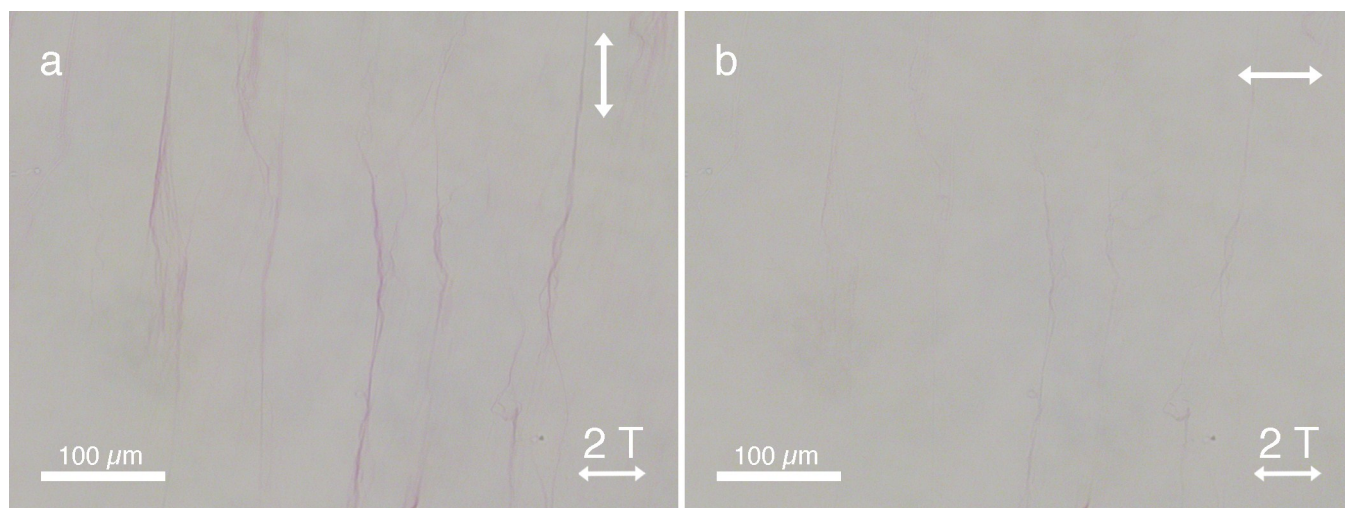


Figure 3. Microscopy images of **PA** (0.026 wt%) in DSCG (13.7 wt% in milli-Q) after alignment in a 2 T magnetic field, showing a strong dichroic response. The temperature of the sample was raised to 65 °C (isotropic phase of DSCG) to remove dichroic contribution from the DSCG birefringence. The double-sided white arrows in the top right corner indicate the orientation of the polarizer in the OM stage. When the polarizer is aligned along the backbone of the **PA** assemblies (a) light is strongly absorbed due to the aligned π -conjugated backbones. When the polarizer is oriented perpendicular to the backbones of the **PA**, light absorption is reduced (b). Due to the increased temperature, the **PA** bundles undergo a color change from blue to red.

Figure 4 schematically displays the templating mechanism responsible for macroscopic **PA** alignment. At high temperatures (> 80 °C) both **PA** (grey, Figure S7) and DSCG⁴⁹ (yellow) are (mostly) molecularly dissolved (Figure 4a). Cooling to 50 °C initiates self-assembly of **PA** fibers, which are not responsive to the 2 T magnetic field thus orient isotropically (Figure 4b). Simultaneously during cooling, the self-assembled DSCG stacks have grown long enough to form nematic LCLC domains wherein the stacks align perpendicular to the magnetic field (Figure 4c) as a result of their negative diamagnetic anisotropy. The presence of **PA** bundles may facilitate LCLC formation (Figure S8) since we observed a slight increase (from 32.7 to 33.7 °C) in the clearing temperature of DSCG (13.4 wt%) with **PA** present. Whilst the LC domains expand into a single monodomain, reorienting shear forces and elastic mediated forces direct the alignment of **PA** nanofibers parallel to the LCLC template (Figure 4d). Meanwhile during the cooling process, depletion interactions with the LCLC solvent forces these nanometer-wide fibers to form much thicker bundles (Figure 4e, Figure S9). After photopolymerization, the **PA** assemblies are very stable due to the crosslinked diacetylene cores which are oriented parallel to the fiber's long axis (indicated by the vertical dark blue line in the inset in Figure 4f). Due to the increased stability, the template can be readily removed. In addition, the **PA** bundles show strong linear polarized absorption characteristics because of the presence of a transition dipole moment parallel to the π -conjugated polydiacetylene **PA** backbones.

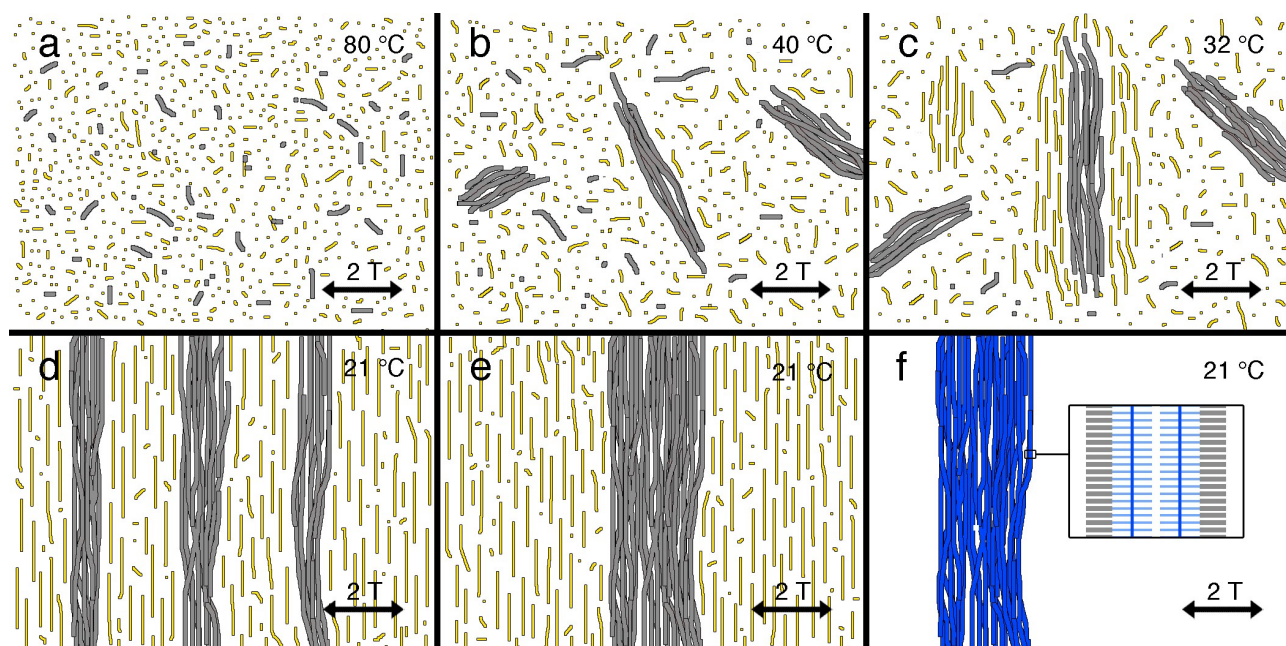


Figure 4. Cartoon of the mechanism of LCLC (yellow) templated PA (grey) alignment in low (2 T) magnetic fields. Cooling the sample from a molecularly dissolved PA and DSCG solution at high temperatures (panel a) first leads to PA assembly which are not affected by the small magnetic field (panel b). At slightly lower temperatures, we find the DSCG transition into the nematic-isotropic biphasic regime. The nematic droplet (in an isotropic continuum) are aligned by the 2 T field and the PA in them will be reoriented by the liquid crystalline matrix (panel c). Further cooling increases the fraction of (aligned) nematic DSCG solution until at room temperature a continuous nematic phase is formed. At the same time, the PA monomers continue to assemble into increasingly long fibres. As their environment now is homogeneously aligned (panel d), we find full efficient templating to the PA assemblies. Keeping the sample at room temperature results in a further (lateral) assembly process of the PA fibres (panel e). At this stage, the fibres can be photopolymerized (blue colored fibers) and the template can be removed (panel f). The inset in panel f shows the position of the individual PA monomers with respect to the bundle's long axis. The dark blue vertical bar indicates direction of the π -conjugated backbone after photopolymerization.

Hierarchically patterned π -conjugated peptide amphiphiles

Besides utilizing a template to realize macroscopic unidirectional peptide amphiphile orientation, we used the orthogonal diamagnetic anisotropies of DSCG and PA to create complex hierarchical PA structures in high magnetic fields. At these high fields, we anticipated a competition between the two PA alignment forces: the LCLC templates that directs the orientation perpendicular to the magnetic field and the (high) magnetic field itself, which forces the PA stacks to organize parallel to the field.

Sealed glass cells containing PA (0.026 wt%) and DSCG (13.7 wt% in milli-Q) were placed in a high magnetic field setup. The glass cells were heated to 80 °C and a 20 T magnetic field was applied. After cooling the cells to room temperature, the magnetic field was switched off and the sample was studied with (polarized) optical microscopy (**Figure 5**).

Surprisingly, we observed complex LC director fields (Figure 5a) as well as areas of large single domains in the range of several millimeters (Figure 5b). In contrast, when DSCG was aligned in the absence of PA (Figure S10) in a high magnetic field, a perfectly aligned monodomain was obtained. Upon closer inspection with optical microscopy (Figure 5c), we observed two distinct organizations

of fibrous aggregates present everywhere in the sample: (i) fibers aligned parallel to the direction of the applied magnetic field, sometimes in conjunction with spindle-like structures (aligned perpendicular to the field); and (ii) fibers aligned perpendicular to the field in both bundle- and spindle-like formations, identical to the assemblies found after applying a 2 T magnetic field sweep (Figure 2).

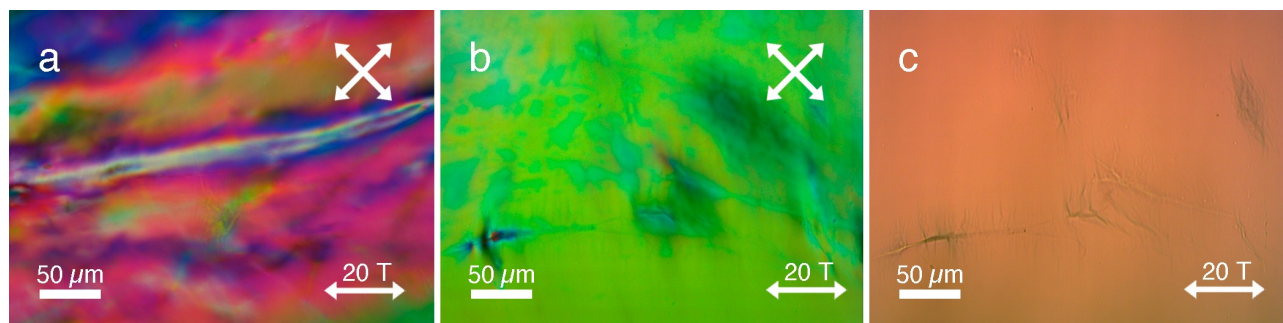


Figure 5. Microscopy images of **PA** (0.026 wt%) in a nematic DSCG template (13.7 wt% in milli-Q) after 20 T magnetic field alignment. POM image (a) shows complex in-plane nematic LCLC director orientations. POM image (b) shows large single LCLC domain, where (after removal of polarizers from POM stage) aligned **PA** aggregates are visible aligned both perpendicular and parallel to the magnetic field (c).

After a photopolymerization step, the orthogonally aligned **PA** assemblies turned blue in color (Figure 5c), analogous to the assemblies in Figure 2. After the cross-linking step, the glass cells were opened and the LCLC was washed away. We used SEM (**Figure 6**) to investigate the hierarchical structures with the two distinct organizations at higher magnifications in order to unravel its morphology. Figure 6a,b and c shows aligned fibrous bundles oriented parallel to the field, in conjunction with perpendicularly aligned spindle-like aggregates. In some locations (Figure 6d), only spindle-like aggregates were found (oriented perpendicular to the magnetic field) without any conjoined bundles that were aligned parallel to the field. These structures are also visible with optical microscopy (Figure 5c, top right corner) and are identical to the assemblies found after a 2 T magnetic field sweep (Figure 2).

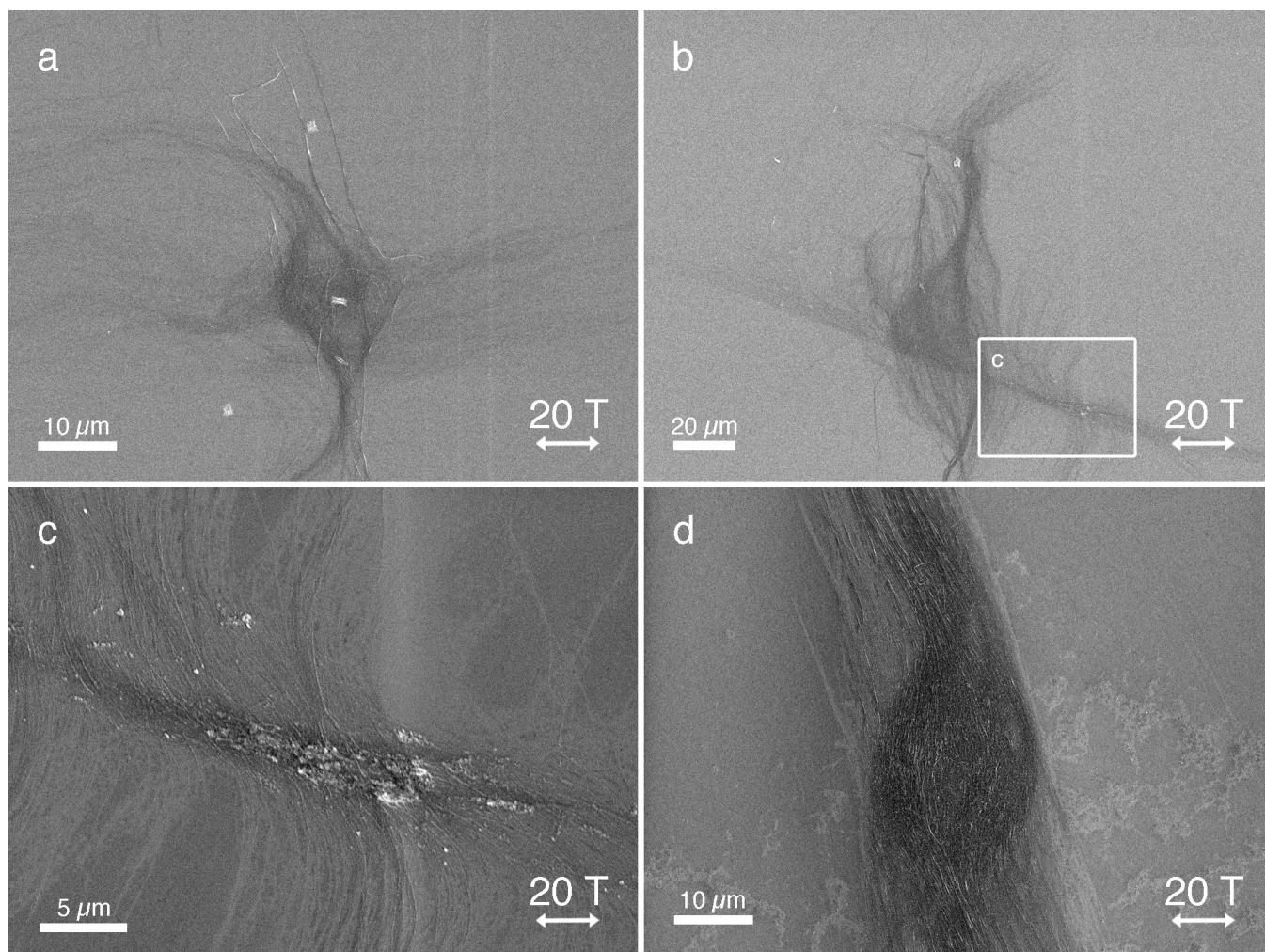


Figure 6. SEM images of PA (0.026 wt%) in a nematic DSCG template (13.7 wt% in milli-Q) after alignment in a 20 T magnetic field. SEM Images (a,b) show orthogonally aligned PA assemblies with fibers oriented both perpendicular and parallel to the magnetic field. Image (c) shows unraveled fibers (perpendicular aligned to the field) from the thicker unidirectionally aligned bundle (parallel to the field). Image (d) shows a unidirectionally aligned spindle similar to a 2 T aligned PA bundle (Figure 2c).

We postulate that these two distinct PA fiber orientations actually are the result of competition in alignment introduced by the positive diamagnetic susceptibility of PA and perpendicular alignment along the LCLC template induced by its negative diamagnetic susceptibility.⁵²

Figure 7 schematically shows the prime processes cooling from the molecularly dissolved state at 80 °C (Figure 7a) in the presence of a high (20 T) magnetic field. Again at approximately 50 °C, PA fiber (grey) formation commences which now is directed by the strong magnetic field (Figure 7b), yielding bundles parallel to the field. Due to the time and temperature-dependent depletion interactions and the ongoing PA assembly, these fibers continue to grow in dimensions (Figure 7c). Simultaneously during cooling, small nematic DSCG domains form and grow to eventually form large nematic domains throughout the sample. Newly formed and still dissolved PA fibers may now follow the elastic forces induced by the nematic DSCG phase and orient perpendicular to the fibers that are already present before. They may give rise to new bundles that are entirely aligned

perpendicular to the field (Figure 6a) or associate tangentially to the existing parallel bundles (Figure 6a,b,c and 7d).

The elastic forces are not high enough to reorient large **PA** bundles, which maintain their parallel orientation. One should consider, however, that phase formation in DSCG sets in at a lower temperature than **PA** assembly. The fact that we see significant amounts of perpendicularly oriented **PA** fibers suggests that the elastic forces are stronger than the magnetic forces (at 20 T). This is supported by the observation of tiny fibers emerging from the large parallel aligned bundles that unravel and predominantly bend in the direction of the nematic LCLC template (Figure 6c). These assemblies then act as a nucleation point for further **PA** assembly and bundling until room temperature is reached (Figure 7e).

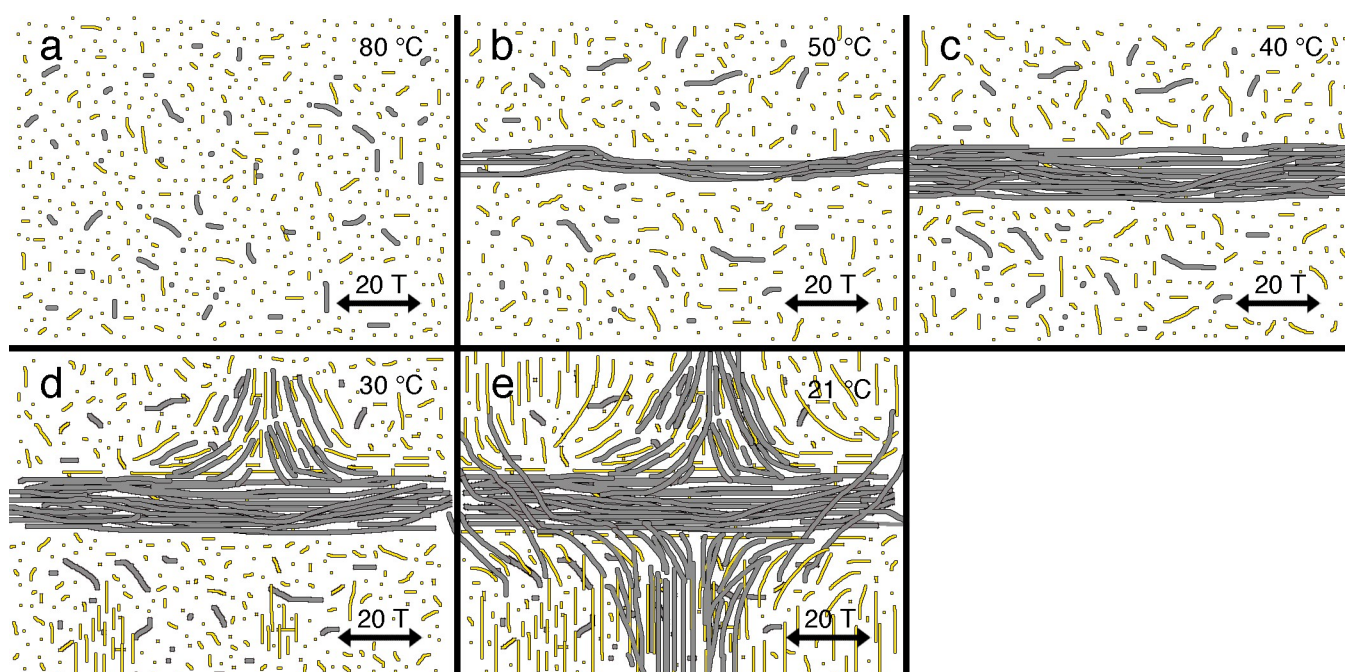


Figure 7. Cartoon of the mechanism of LCLC (yellow) templated **PA** (grey) alignment in high (20 T) magnetic fields, again starting from a high temperature solution with DSCG and **PA** molecularly dissolved (panel a). Upon cooling the sample, **PA** fibres start forming first. In the 20 T magnetic field, these fibres start growing parallel to the field (the monomers with negative $\Delta\chi$ perpendicular to the field) and expanding (panels b,c). At the clearing temperature of the DSCG solution, nematic droplets form, in which the DSCG aggregates are oriented perpendicular to the field. These droplets and, at lower temperatures, the homogeneously aligned DSCG solution will then template further **PA** fibre growth in the direction of the nematic matrix and thus perpendicular to early formed fibres.

When conducting the same experiment at a lower magnetic field of 15 T, **PA** neither formed assemblies that aligned parallel to the field nor orthogonal bundled aggregates. Instead, only homogeneously aligned structures as in Figure 2 and Figure 6d (perpendicular to the magnetic field direction and parallel to the DSCG stacks) were observed (Figure S11a,b). We found similar **PA** aggregates (again perpendicular to the field) when **PA** was assembled at lower concentrations (0.013 wt%) in a DSCG template at 20 T (Figure S11c). Apparently, at these lower concentrations the assembly of **PA** is dominated by the LCLC template despite the presence of the high magnetic

field. On the other hand, at increased **PA** concentrations (0.039 wt%), the orthogonal structures similar to the ones in Figure 5c and Figure 6a,b were observed (Figure S11d). The higher **PA** concentrations result in the formation of larger assemblies which in turn have an increased diamagnetic susceptibility and hence an increased responsiveness to the magnetic field.⁴⁸ This is further supported by control experiments which show that 0.1 wt% **PA** (without DSCG present) assembled at 20 T form macroscopic aligned bundles along the magnetic field direction, while at 0.015 wt% **PA** (without DSCG present) at 20 T no macroscopic alignment is observed (Figure S12). Overall, the structure formation of these supramolecular materials in LCLC templates and magnetic fields depends on the relative strengths of the two opposing contributions, which both can be tuned independently. The shear and elastic forces of the template can be tailored by the particular LCLC used, as well as the temperature and concentration of the template. The diamagnetic susceptibility of **PA** can be tuned by its concentration and also the temperature. In addition, the magnetic field itself is an important parameter as is the (temperature, time and concentration dependent) depletion effect. A more detailed understanding of all of these factors will be the starting point to control and utilize the complex structures that are available through these methods.

Conclusion

In this work, we show that we can create unidirectional aligned arrays of functional supramolecular materials on a centimeter scale by combining LCLC templates with 2 T magnetic fields. After photopolymerization, these materials show strong linear polarized absorption characteristics due to the macroscopic aligned π -conjugated backbones. Their increased mechanical strength also allows for the removal of the LCLC template by a simple washing step, leaving the optically active amphiphiles unidirectionally aligned on the substrate. With this approach it is possible to align these materials at 10 times lower magnetic field strengths than previously reported.¹⁸

This approach has the great advantage that it can be applied to macroscopically align a wide range of soft matter, since the alignment procedure solely relies on orientational shear and elastic forces and lacks the requirement for delicate molecular interactions that require fine tuning. Since we are also able to drastically lower the requirements for magnetic field alignment with this approach, we envisage the use of small commercially available permanent magnets, for instance based on neodymium, integrated within tabletop setups for applying this technique to a huge number of aqueous functional soft materials.

Additionally, the reduction of the field required for alignment opens up the opportunity to create more complex structures at much higher fields. We created orthogonally aligned **PA** assemblies by exploiting the opposite diamagnetic anisotropies of our LC template and self-assembled amphiphilic materials. Such self-assembled off-equilibrium structures are impossible to create on such a small length scales using other conventional alignment techniques. We believe, therefore, that this approach is very promising to create tailor-made complex structures of (aqueous)

functional soft matter highly beneficial for device applications in many diverse areas. A better control of the critical parameters that we set out in the manuscript will be necessary to achieve this.

Acknowledgements

We would like to thank both Britta Ramakers and Dennis Löwik for the synthesis of **PA** and the TechnoCentrum for the fabrication of the cell construction apparatus.

This work is supported by NanoNextNL (PvdA, PHJK, grant 07A.07 & MK, grant 07A.06), a micro and nanotechnology consortium of the Government of the Netherlands and 130 partners.

Part of this work is supported by EuroMagNET II under the EU Contract No. 228043. We acknowledge the support of the HFML-RU/FOM, member of the European Magnetic Field Laboratory (EMFL).

References

- 1 M. Gerard, A. Chaubey and B. D. Malhotra, *Biosens. Bioelectron.*, 2002, **17**, 345–359.
- 2 N. K. Guimard, N. Gomez and C. E. Schmidt, *Prog. Polym. Sci.*, 2007, **32**, 876–921.
- 3 S. Cosnier and M. Holzinger, *Chem. Soc. Rev.*, 2011, **40**, 2146–2156.
- 4 F. J. M. Hoeben, P. Jonkheijm, E. W. Meijer and A. P. H. J. Schenning, *Chem. Rev.*, 2005, **105**, 1491–1546.
- 5 L. C. Palmer and S. I. Stupp, *Acc. Chem. Res.*, 2008, **41**, 1674–1684.
- 6 T. Aida, E. W. Meijer and S. I. Stupp, *Science*, 2012, **335**, 813–817.
- 7 B. Su, Y. Wu and L. Jiang, *Chem. Soc. Rev.*, 2012, **41**, 7832–7856.
- 8 Z. Nie and E. Kumacheva, *Nat. Mater.*, 2008, **7**, 277–290.
- 9 H. M. Saavedra, T. J. Mullen, P. Zhang, D. C. Dewey, S. A. Claridge and P. S. Weiss, *Rep. Prog. Phys.*, 2010, **73**, 036501.
- 10 B. D. Gates, Q. Xu, M. Stewart, D. Ryan, C. G. Willson and G. M. Whitesides, *Chem. Rev.*, 2005, **105**, 1171–1196.
- 11 D. Li, Y. Wang and Y. Xia, *Adv. Mater.*, 2004, **16**, 361–366.
- 12 D. Yang, B. Lu, Y. Zhao and X. Jiang, *Adv. Mater.*, 2007, **19**, 3702–3706.
- 13 A. S. Tayi, E. T. Pashuck, C. J. Newcomb, M. T. McClendon and S. I. Stupp, *Biomacromolecules*, 2014, **15**, 1323–1327.
- 14 M. Wang, L. Du, X. Wu, S. Xiong and P. K. Chu, *ACS Nano*, 2011, **5**, 4448–4454.
- 15 L. Sardone, V. Palermo, E. Devaux, D. Credgington, M. de Loos, G. Marletta, F. Cacialli, J. van Esch and P. Samori, *Adv. Mater.*, 2006, **18**, 1276–1280.
- 16 Y. Shoji, M. Yoshio, T. Yasuda, M. Funahashi and T. Kato, *J. Mater. Chem.*, 2009, **20**, 173–179.
- 17 M. Yoshio, Y. Shoji, Y. Tochigi, Y. Nishikawa and T. Kato, *J. Am. Chem. Soc.*, 2009, **131**, 6763–6767.
- 18 D. W. P. M. Löwik, I. O. Shklyarevskiy, L. Ruizendaal, P. C. M. Christianen, J. C. Maan and J. C. M. van Hest, *Adv. Mater.*, 2007, **19**, 1191–1195.
- 19 M. van den Heuvel, A. M. Prenten, J. C. Gielen, P. C. M. Christianen, D. J. Broer, D. W. P. M. Löwik and J. C. M. van Hest, *J. Am. Chem. Soc.*, 2009, **131**, 15014–15017.
- 20 M. Wallace, A. Z. Cardoso, W. J. Frith, J. A. Iggo and D. J. Adams, *Chem. Eur. J.*, 2014, **20**, 16484–16487.
- 21 P. van der Asdonk, H.C. Hendrikse, M.F.-C. Romera, D. Voerman, B.E.I. Ramakers, D.W.P.M. Löwik, R.P. Sijbesma, P.H.J. Kouwer, *Adv. Funct. Mater.* 2016, **26**, 2609–2616.
- 22 T. Kato, Y. Hirai, S. Nakaso and M. Moriyama, *Chem. Soc. Rev.*, 2007, **36**, 1857–2128.
- 23 Y. Hirai, S. S. Babu, V. K. Praveen, T. Yasuda, A. Ajayaghosh and T. Kato, *Adv. Mater.*, 2009, **21**, 4029–4033.
- 24 K. Akagi, G. Piao, S. Kaneko, K. Sakamaki, H. Shirakawa and M. Kyotani, *Science*, 1998, **282**, 1683–1686.
- 25 M. Goh, S. Matsushita and K. Akagi, *Chem. Soc. Rev.*, 2010, **39**, 2466–2476.
- 26 M. D. Lynch and D. L. Patrick, *Nano Lett.*, 2002, **2**, 1197–1201.
- 27 I. Dierking, G. Scalia, P. Morales and D. LeClere, *Adv. Mater.*, 2004, **16**, 865–869.
- 28 O. Catanescu and L.-C. Chien, *Adv. Mater.*, 2005, **17**, 305–309.

- 29 S. Moynihan, P. Lovera, D. O'Carroll, D. Iacopino and G. Redmond, *Adv. Mater.*, 2008, **20**, 2497–2502.
- 30 X. Tong, D. Han, D. Fortin and Y. Zhao, *Adv. Funct. Mater.*, 2012, **23**, 204–208.
- 31 J.-W. Chen, C.-C. Huang and C.-Y. Chao, *ACS Appl. Mater. Interfaces*, 2014, **6**, 6757–6764.
- 32 J. Lagerwall, G. Scalia, M. Haluska, U. Dettlaff-Weglikowska, S. Roth and F. Giesselmann, *Adv. Mater.*, 2007, **19**, 359–364.
- 33 M. Hara, S. Nagano, N. Kawatsuki and T. Seki, *J. Mater. Chem.*, 2008, **18**, 3259.
- 34 N. Ould-Moussa, C. Blanc, C. Zamora-Ledezma, O. D. Lavrentovich, I. I. Smalyukh, M. F. Islam, A. G. Yodh, M. Maugey, P. Poulin, E. Anglaret and M. Nobili, *Liquid Crystals*, 2013, **40**, 1628–1635.
- 35 P. C. Mushenheim, R. R. Trivedi, H. H. Tuson, D. B. Weibel and N. L. Abbott, *Soft Matter*, 2013, **10**, 88.
- 36 S. Zhou, A. Sokolov, O. D. Lavrentovich and I. S. Aranson, *Proc. Natl. Acad. Sci. U.S.A.*, 2014, **111**, 1265–1270.
- 37 P. C. Mushenheim, R. R. Trivedi, D. B. Weibel and N. L. Abbott, *Biophys. J.*, 2014, **107**, 255–265.
- 38 S. Zhang, M. A. Greenfield, A. Mata, L. C. Palmer, R. Bitton, J. R. Mantei, C. Aparicio, M. O. de la Cruz and S. I. Stupp, *Nat. Mater.*, 2010, **9**, 594–601.
- 39 J. B. Matson and S. I. Stupp, *Chem. Commun.*, 2012, **48**, 26–33.
- 40 S. R. Diegelmann, N. Hartman, N. Markovic and J. D. Tovar, *J. Am. Chem. Soc.*, 2012, **134**, 2028–2031.
- 41 M. T. McClendon and S. I. Stupp, *Biomaterials*, 2012, **33**, 5713–5722.
- 42 E. J. Berns, S. Sur, L. Pan, J. E. Goldberger, S. Suresh, S. Zhang, J. A. Kessler and S. I. Stupp, *Biomaterials*, 2014, **35**, 185–195.
- 43 X. Chen, G. Zhou, X. Peng and J. Yoon, *Chem. Soc. Rev.*, 2012, **41**, 4610–21.
- 44 B. E. I. Ramakers, M. van den Heuvel, N. Tsihchlis i Spithas, R. P. Brinkhuis, J. C. M. van Hest and D. W. P. M. Löwik, *Langmuir*, 2012, **28**, 2049–2055.
- 45 B. E. I. Ramakers, S. A. Bode, A. R. Killaars, J. C. M. van Hest and D. W. P. M. Löwik, *J. Mat. Chem. B*, 2015, **3**, 2954–2961.
- 46 B. D. Wall, S. R. Diegelmann, S. Zhang, T. J. Dawidczyk, W. L. Wilson, H. E. Katz, H.-Q. Mao and J. D. Tovar, *Adv. Mater.*, 2011, **23**, 5009–5014.
- 47 A. M. Hung and S. I. Stupp, *Nano Lett.*, 2007, **7**, 1165–1171.
- 48 G. Maret and K. Dransfeld, in *Strong and Ultrastrong Magnetic Fields and Their Applications*, Springer Berlin Heidelberg, Berlin, Heidelberg, 1985, vol. 57, pp. 143–204.
- 49 J. Lydon, *J. Mater. Chem.*, 2010, **20**, 10071–10099.
- 50 V. G. Nazarenko, O. P. Boiko, H. S. Park, O. M. Brodyn, M. M. Omelchenko, L. Tortora, Y. A. Nastishin and O. D. Lavrentovich, *Phys. Rev. Lett.*, 2010, **105**, 017801.
- 51 T. Ostapenko, Y. A. Nastishin, P. J. Collings, S. N. Sprunt, O. D. Lavrentovich and J. T. Gleeson, *Soft Matter*, 2013, **9**, 9487–9498.
- 52 We noticed that a part of the **PA** aggregates bundles are not completely aligned parallel or perpendicular to the magnet field direction (Figure 5c, Figure 6a,b), which we can attribute to the orthogonal alignment forces acting on the organization of bundled **PA** fibers (positive diamagnetic susceptibility versus LCLC template shear and elastic forces) which are in the same order of magnitude. A similar effect was described before in Ref. 26

Manuscript ID: SM-ART-03-2016-000652

TITLE: Directed Peptide Amphiphile Assembly Using Aqueous Liquid Crystal Templates in Magnetic Fields

ToC entry

Controlling structure formation of functional supramolecular materials by using aqueous liquid crystalline templates in magnetic fields.

